



9A



9B



10

Figures 9-10: As-received views of the cylinder showing identification markings on its bottom (figure 9), caution sticker, and date of internal inspection (figure 10).



11, X 0.5 approx.

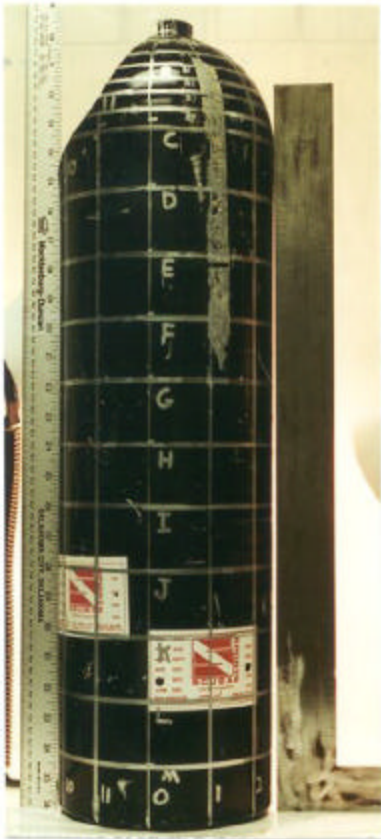


12, X 0.5 approx.

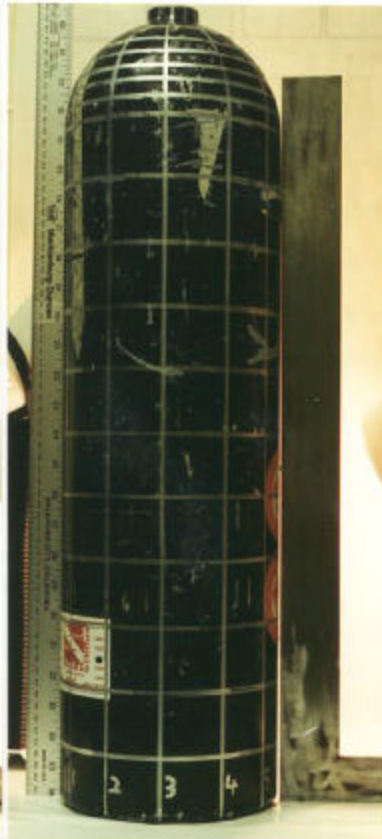


13, X 2 approx.

Figure 11-13: As-received views of two smaller pieces of fracture.



14



15



16



17

Figure 14-17: Photographs exhibiting the grid layout. They also show overall straightness of the cylinders. There appears to be slight bulging near the base of the dome part of the cylinder.



Figure 18A: Locations of chemical samples from near OC grid point (small arrow), and from near OA2 grid point (large arrow).

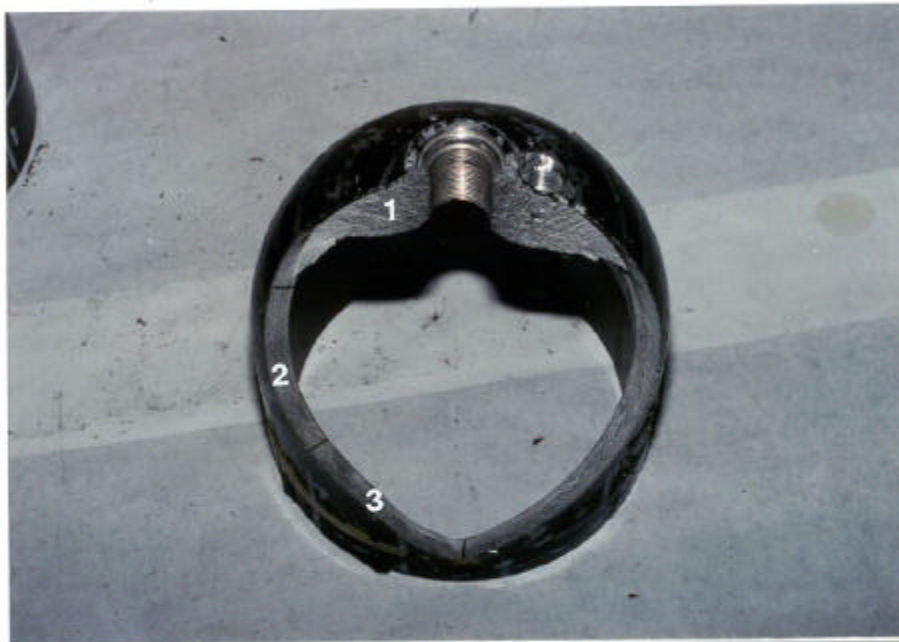


Figure 18B: View of the fractured dome part cut from the cylinder. It shows locations of fracture surface sections 1, 2 and 3, which were removed for examination.



Figure 19: A macro view of the fracture surface. Side A was used for fractography and side B for metallography.



Figure 20: An enlarged view of section 1 (figure 18B) shows three distinct regions on the fracture surface marked A, B and C.

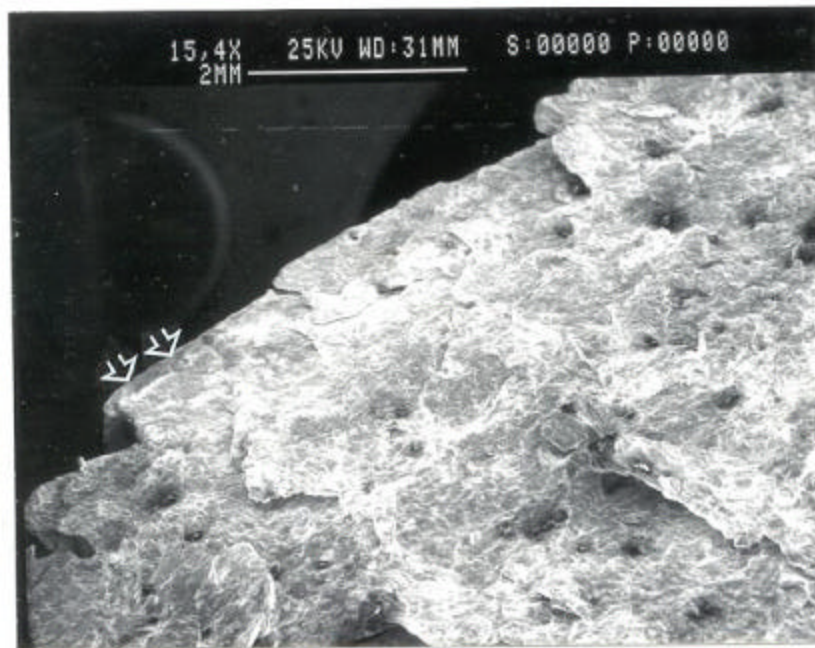


Figure 21: A low magnification SEM fractograph of region A shows areas near the last thread, X15.

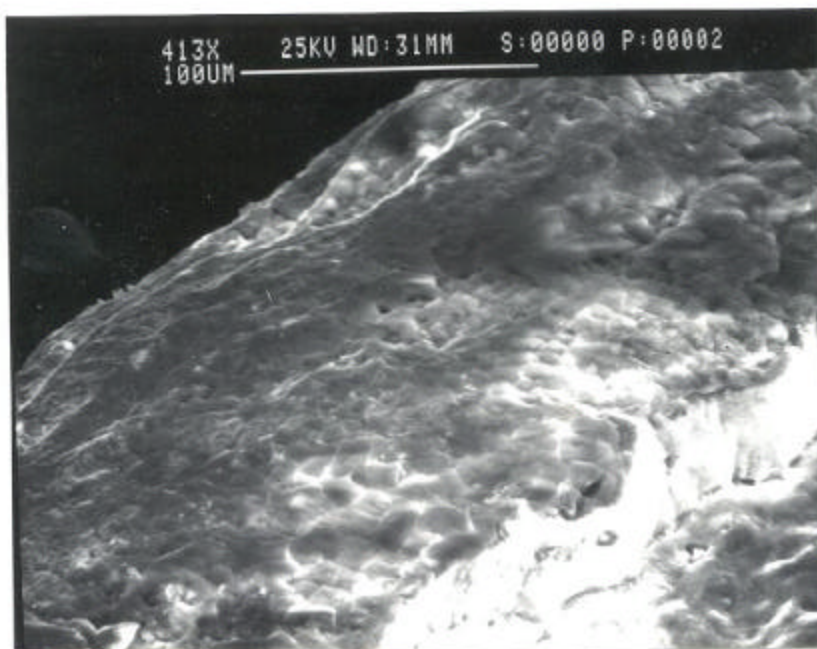


Figure 22: Enlarged view of the edge indicated by arrows in Figure 21, exhibits a featureless metal fold formed during extrusion process, X413.



Figure 23: Fractograph of an area deeper in region A shows featureless fracture. Some evidence of dimpled rupture and intergranular failure was also observed, X832.

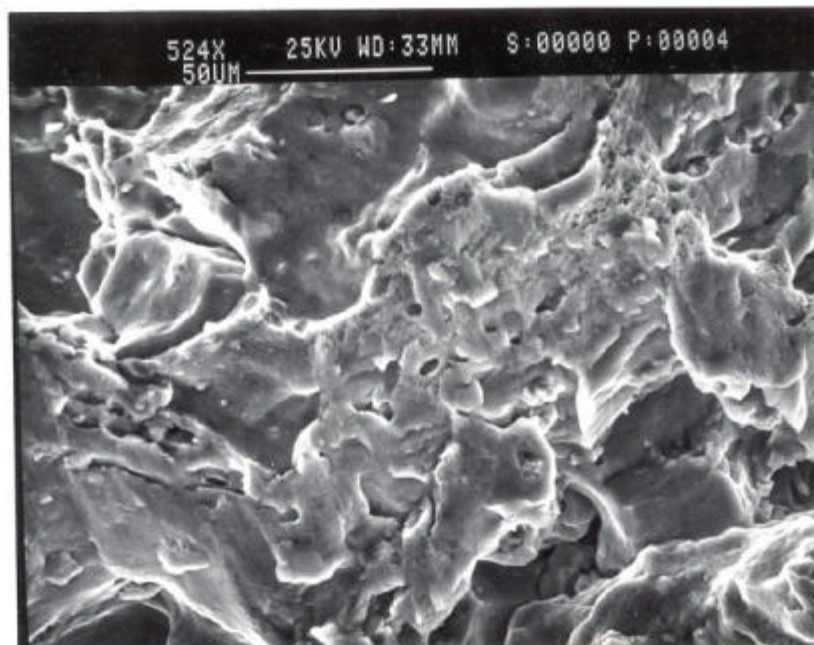


Figure 24: Fractograph from an area in region A (near region B) is featureless as in figure 23. However, evidence of dimpled rupture and grain boundary decohesion is more discernible, X524.



Figure 25: Fracture in region B exhibited featureless regions. It also clearly indicated evidence of grain boundary failure, X663.

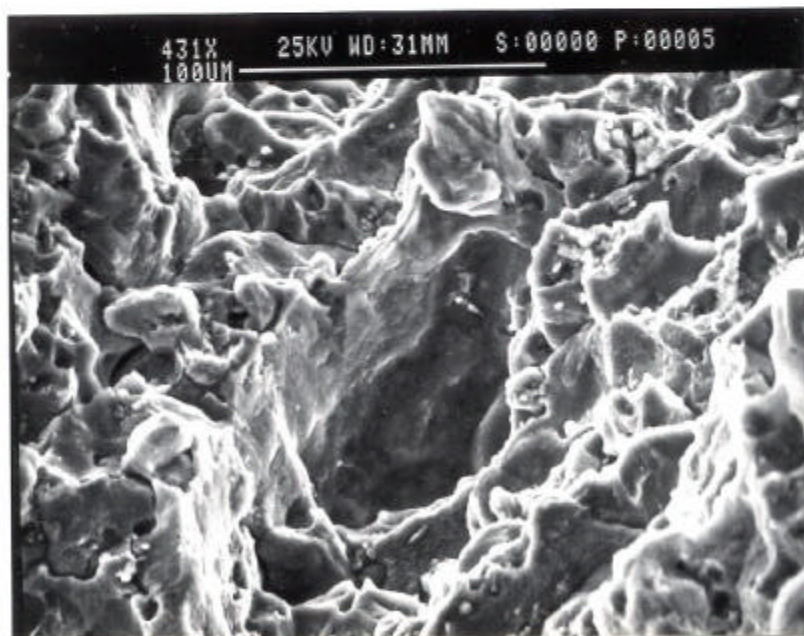


Figure 26: Fractograph from an area in region C. It shows similar features as in figure 24.

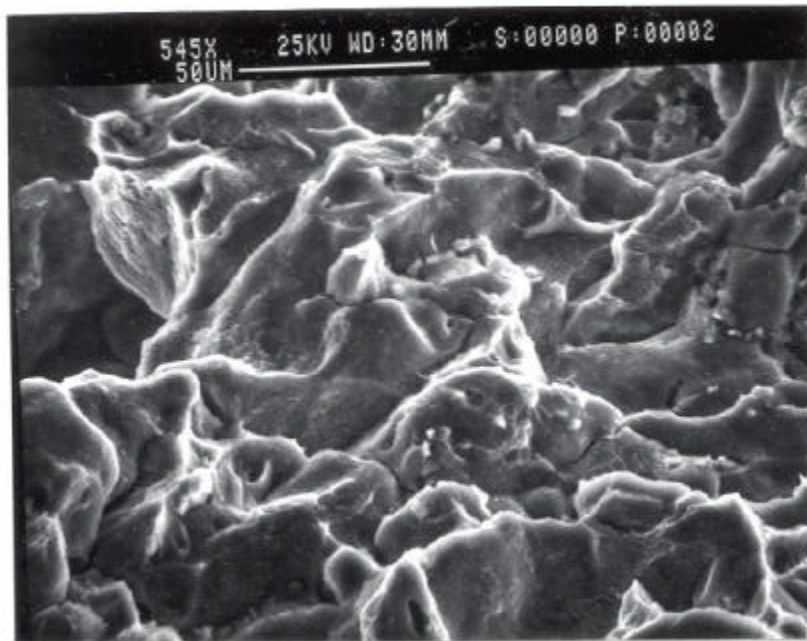


Figure 27: Fractograph from an area deeper in region C. It exhibits clearly defined intergranular failure, X545.

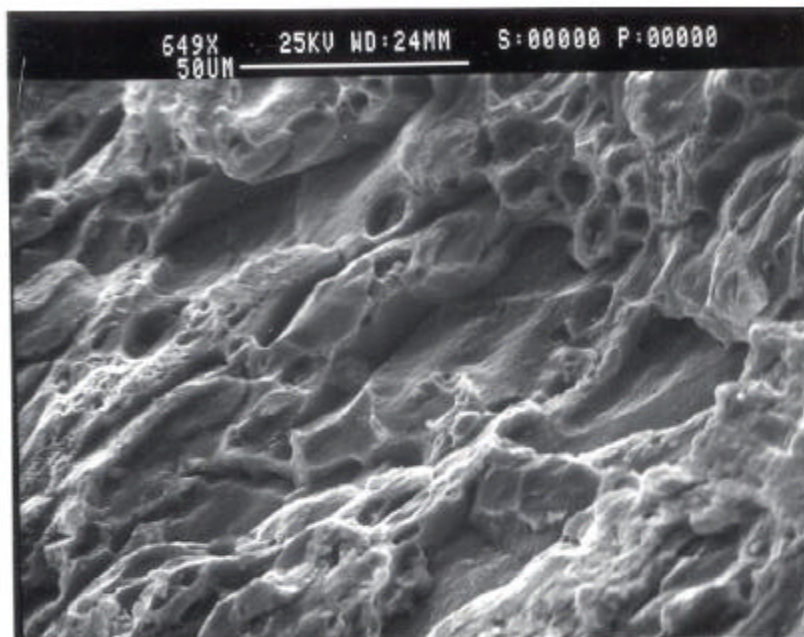


Figure 28: A typical fractograph of the fracture surface in sections B and C showing largely intergranular failure. Some evidence of dimpled failure can also be observed, X649.

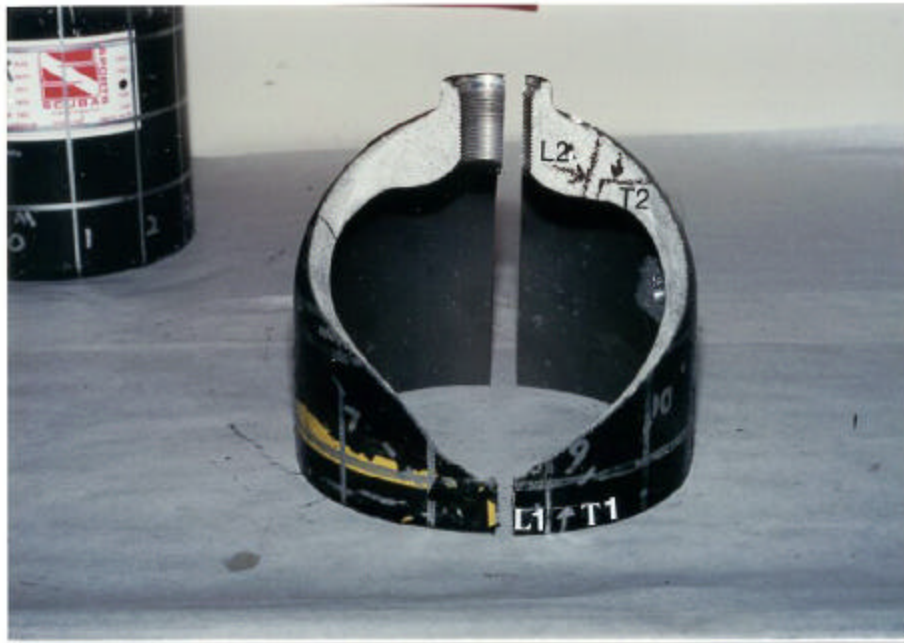


Figure 29: Locations of longitudinal (L1 and L2) and transverse (T1 and T2) sections cut for metallographic examination, shown by arrows.

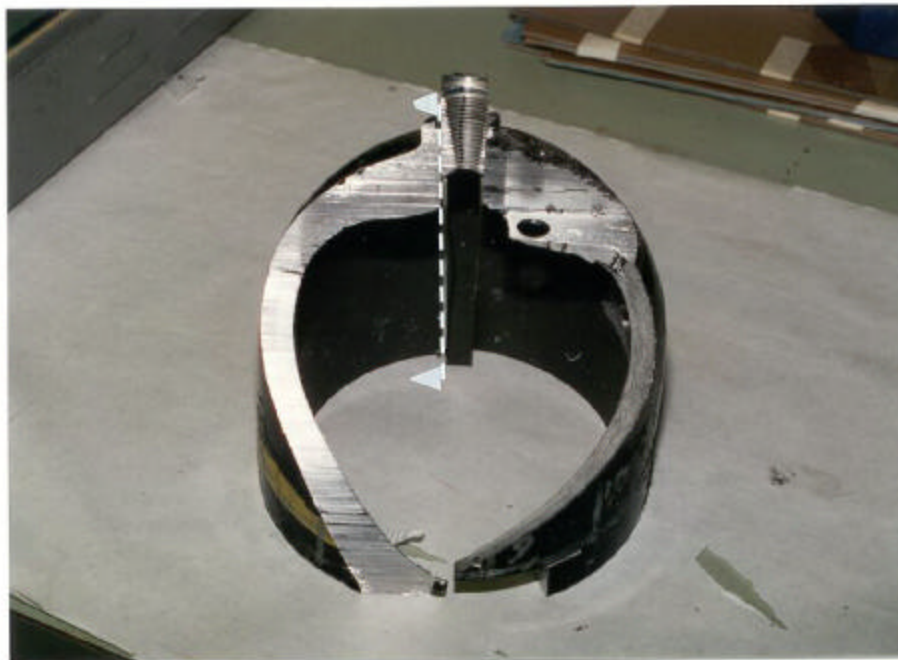


Figure 30: Photograph indicating the section used for macro analysis.

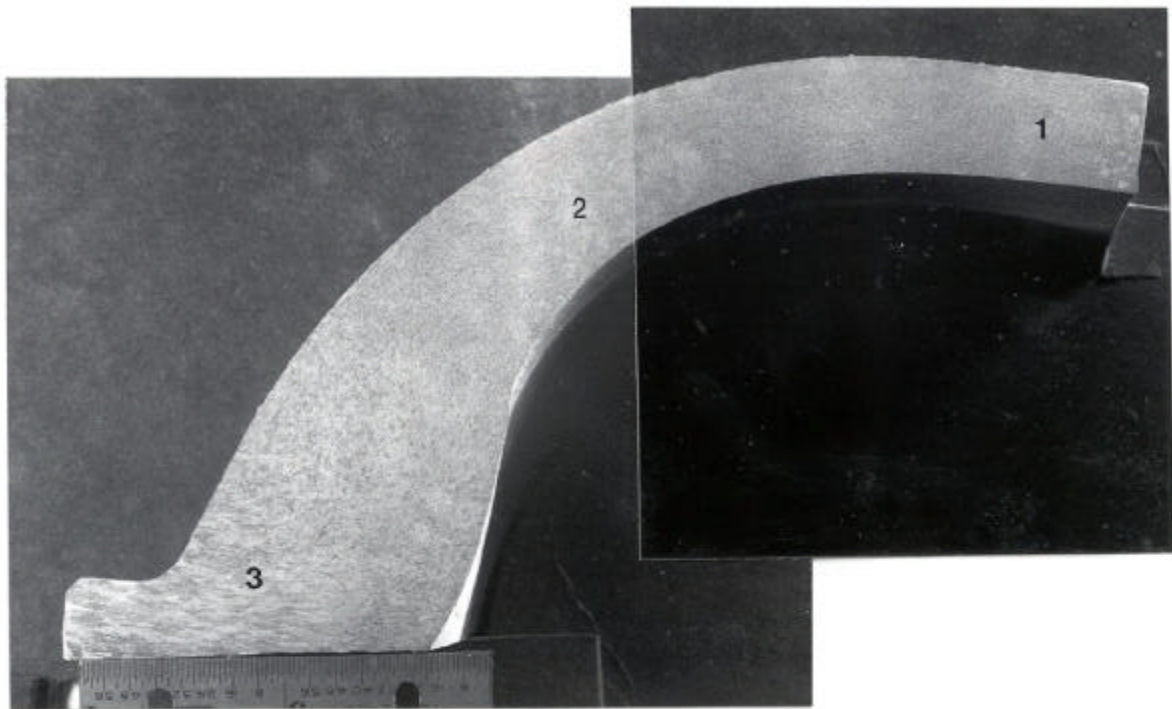
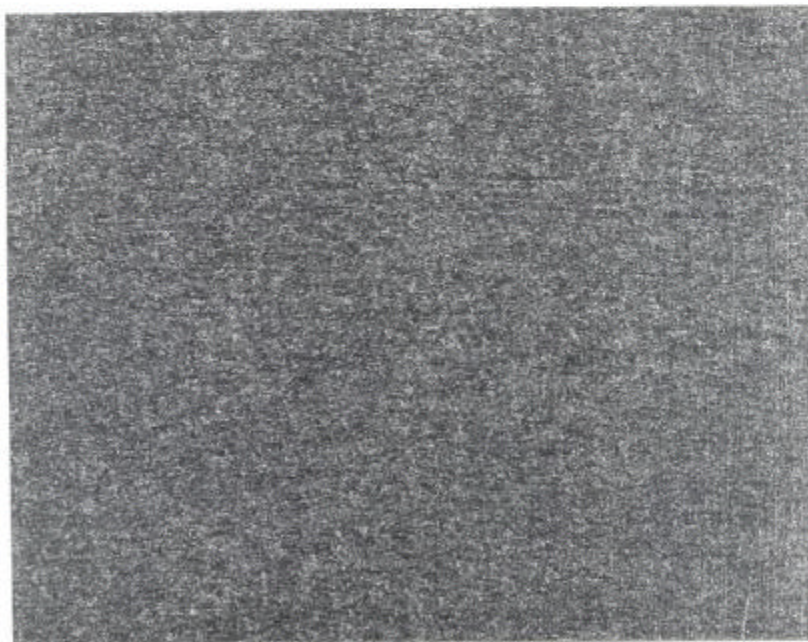


Figure 31: Macrograph of the section indicated in figure 30. It exhibits fine grain structure in the barrel section and coarse grains near the neck region, X1.14, Keller's Etch.



Section 32: Enlarged view of the area marked 1 in figure 31 shows a very fine grain size, X10.